Microstructure-Processing-Microstructure Relationships in Cold Spray Deposited Stainless Steel Coatings

Luke N. Brewer, J.F. Schiel, E.S.K. Menon, and D.J. Woo

Naval Postgraduate School

CSAT-2014

Mr. R. Hays, OSD-Corrosion Policy and Oversight/Dr. K. Ho, NAVFAC-EXWC

Prof. Brewer's Research:

Cold Spray Deposition for Structural Repair and Manufacturing

Al-Nanodiamond composites for high strength/light weight armor

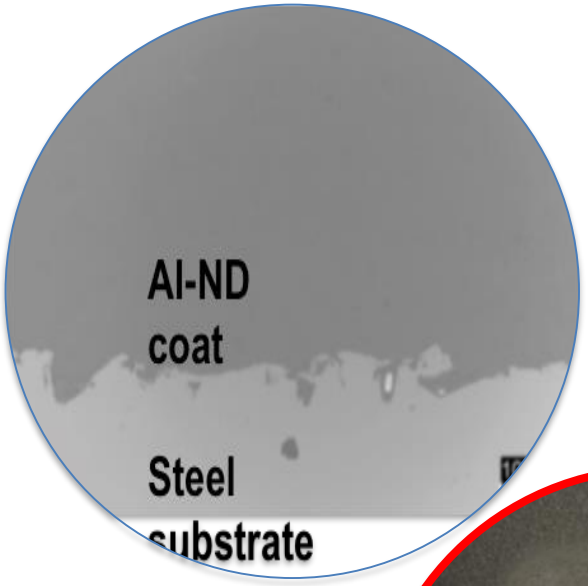

Cold spray of Al-Cu binary alloys to understanding alloying effects

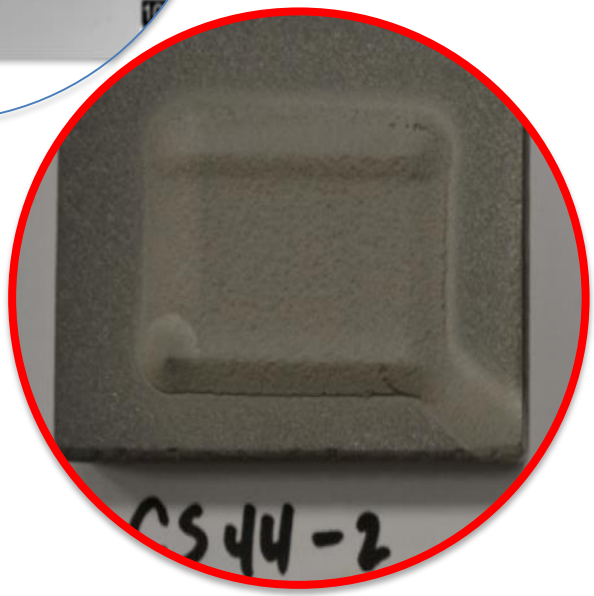

Stainless steel coatings for structural repair and corrosion prevention

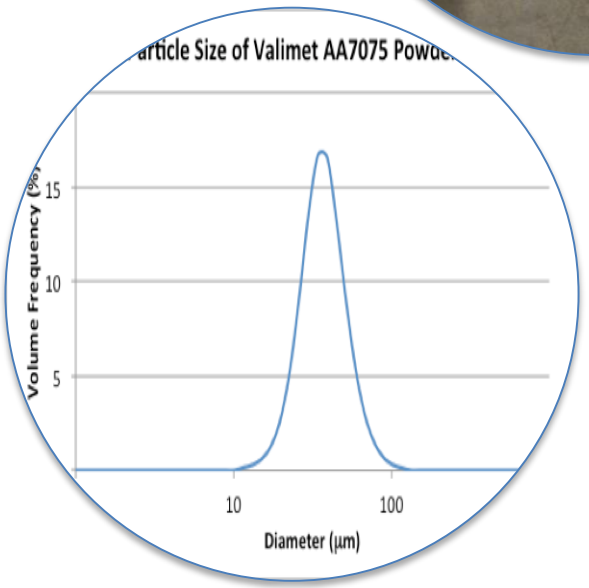

Cold spray of AA7075 for aircraft corrosion prevention and repair

The Problem: can we repair large metallic structures in place?

- Crack in Drydock thimble:
- Location: Pearl Harbor Naval Shipyard
- Constructed in 1919. discharge thimble is component of the dewatering system to pump water out of the drydock.

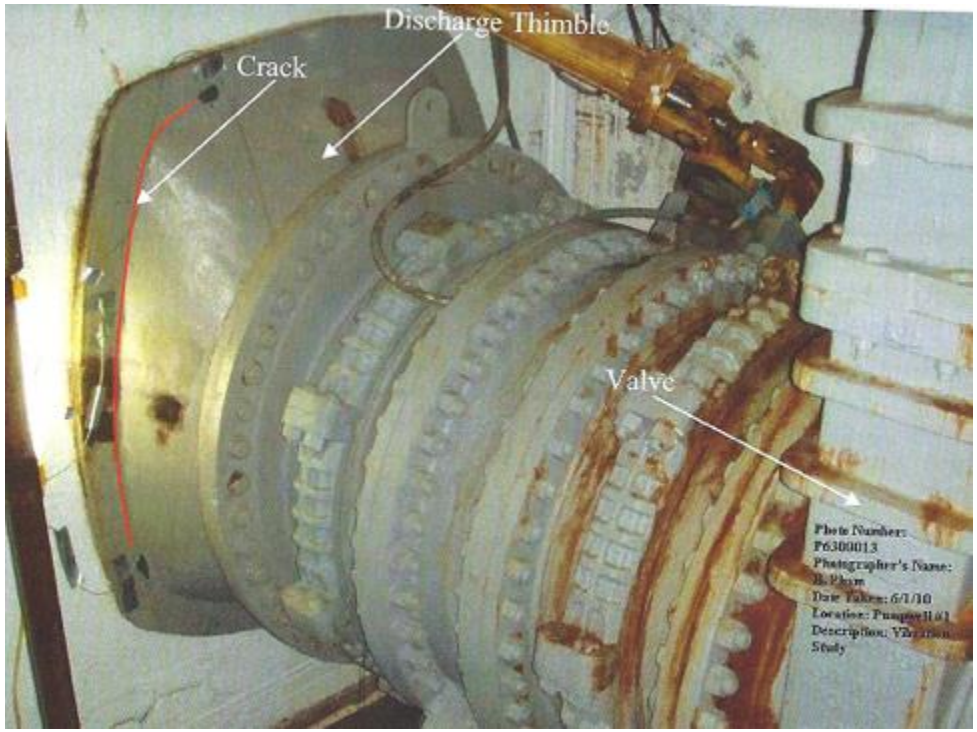

Can we deposit restorative/protective austenitic stainless steel onto damaged structures (e.g. cast iron)?

What do we already know about cold spray of austenitic stainless steels?

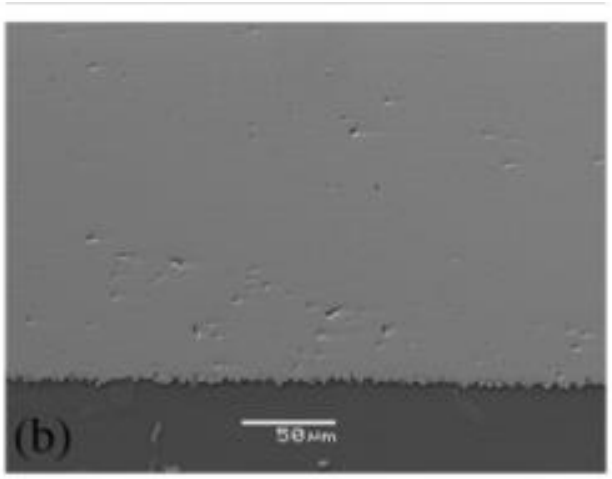

SEM image of austenitic stainless steel CS coating,
from Spencer et al., Surf. Coat. Tech, 2011

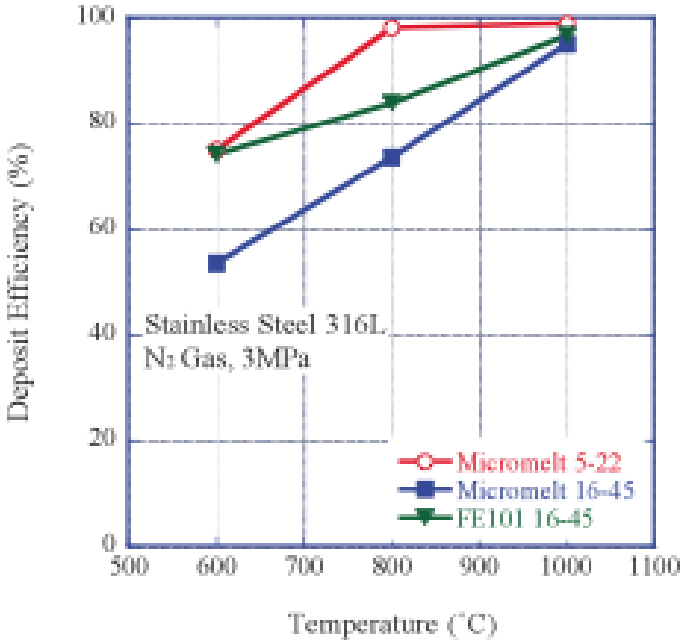

from Huang et al. , Thermal Spray Conf., 2012

We can successfully cold spray 304 and 316SS over a range of temperatures and pressures. Higher pressures, temperatures result in higher DE and less porosity (higher velocity) There may be some ferrite phase in the powder. Minimal mention of ferrite phase in the coating…

What Is the microstructure of the powders? Does it matter? What is the microstructure of the coatings: crystallite size, phase distribution, level of plastic strain?

Cold Spray of Four Commercial Stainless Steel Powders

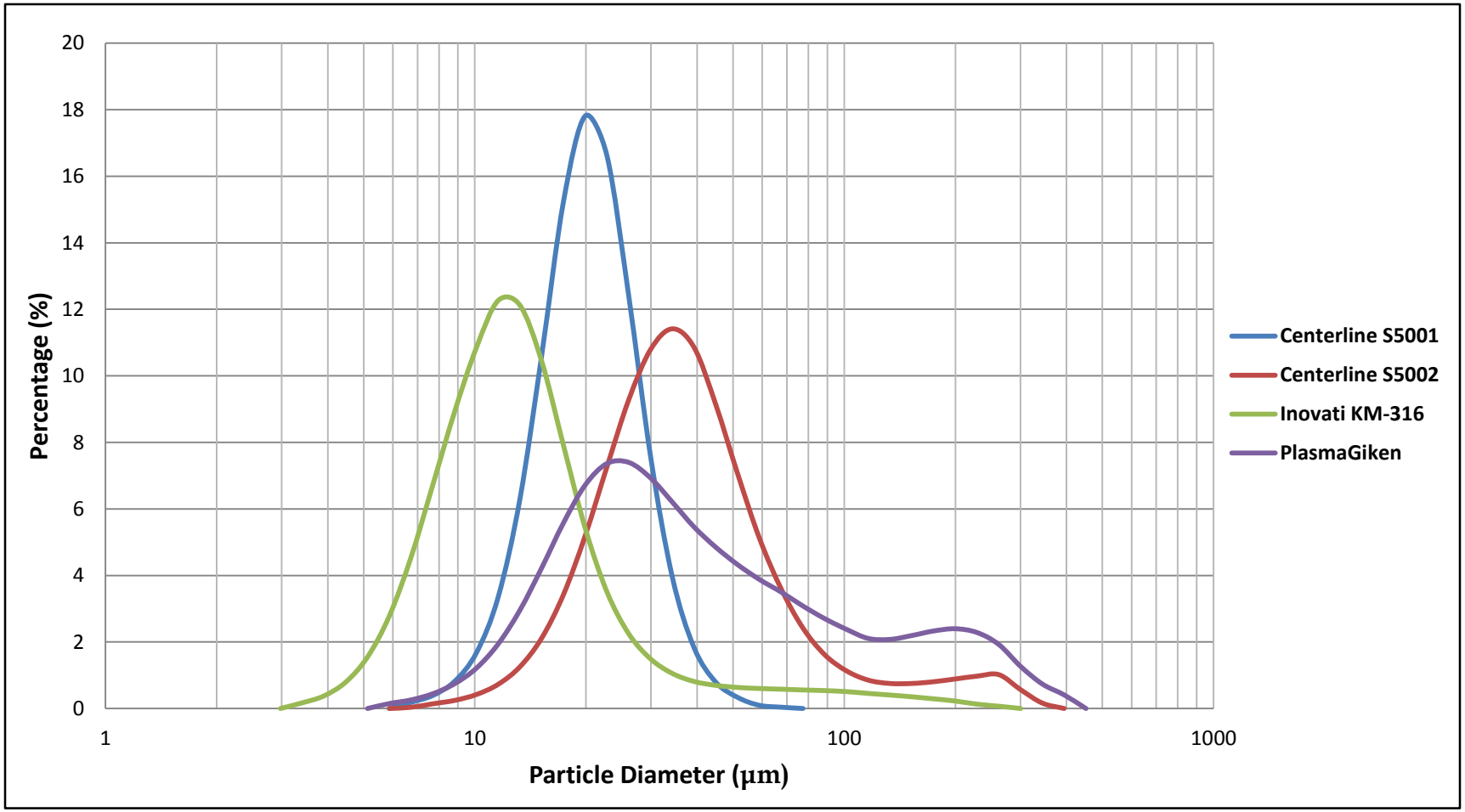

Powder	Mean (µm)	D10 (µm)	D90 (µm)
Centerline S5001 (304L)	19.9	12.5	28.4
Centerline S5002 (316L)	45.6	18.1	75.2
Inovati KM-316 (316L)	17.2	6.7	25.5
Plasma Giken (316L)	61.3	14.3	164.8

External Powder Morphology

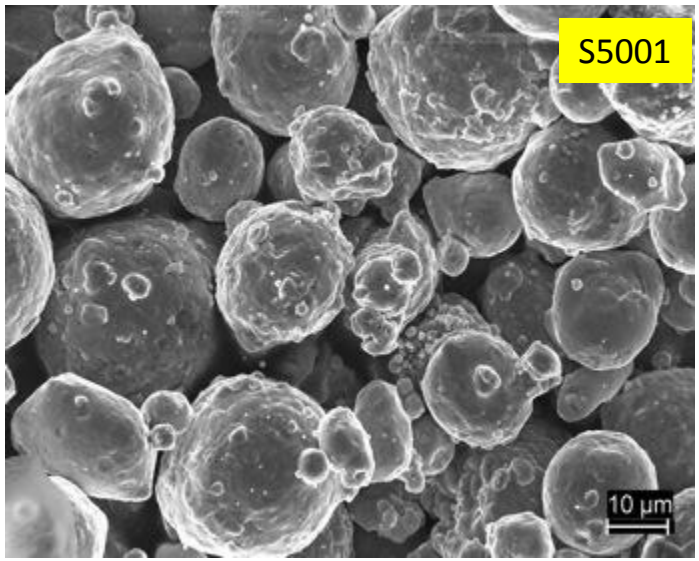

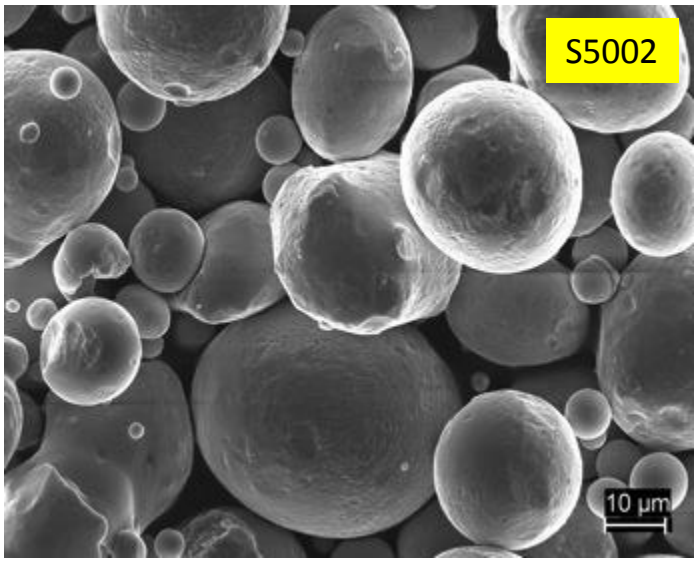

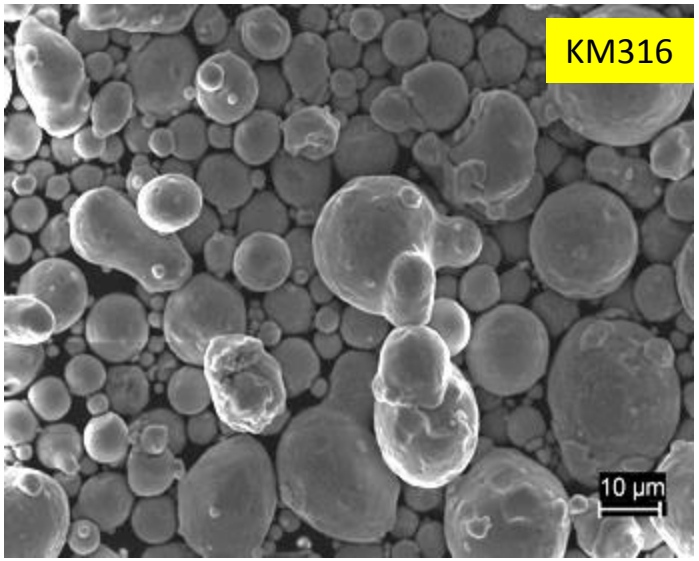

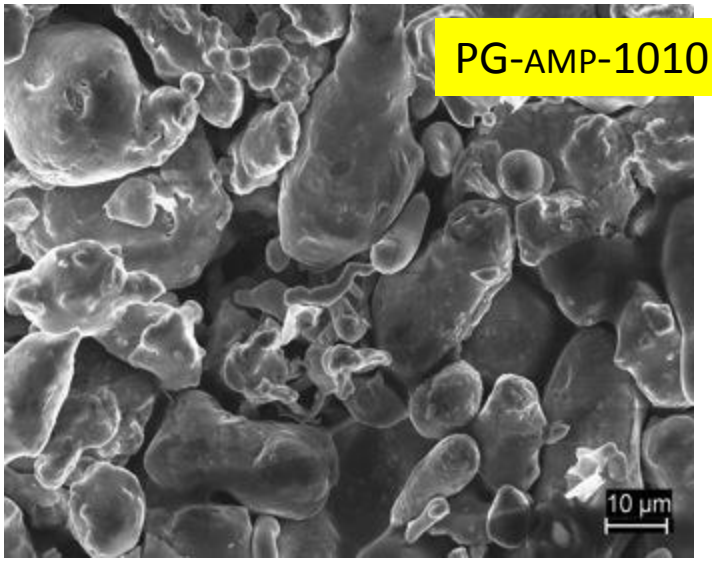

Internal Structure of Particles…

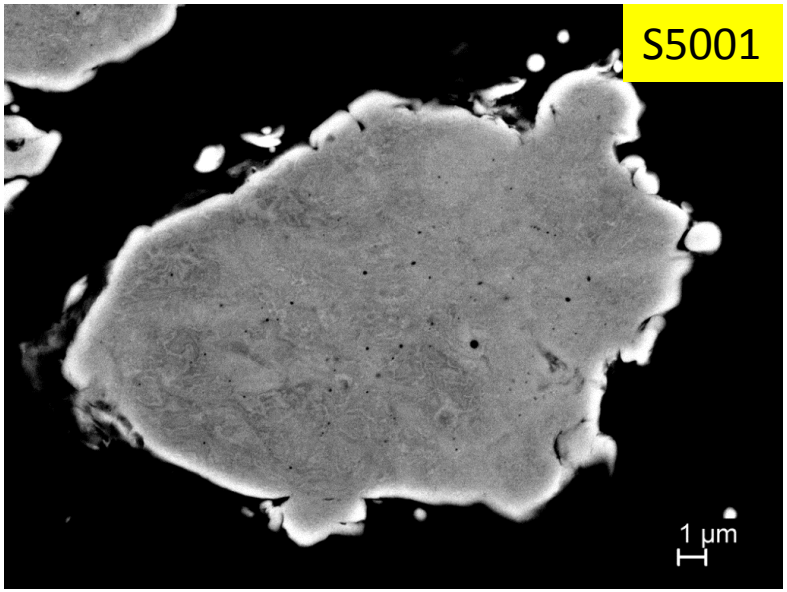

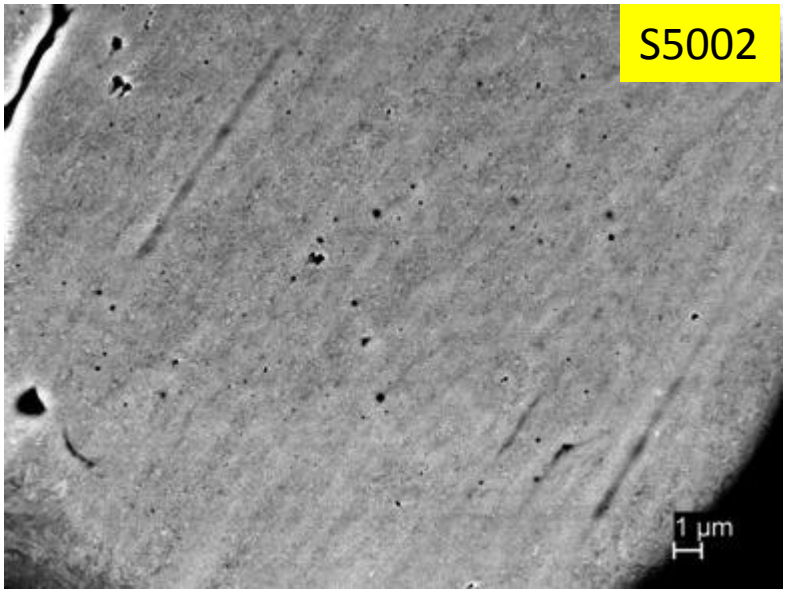

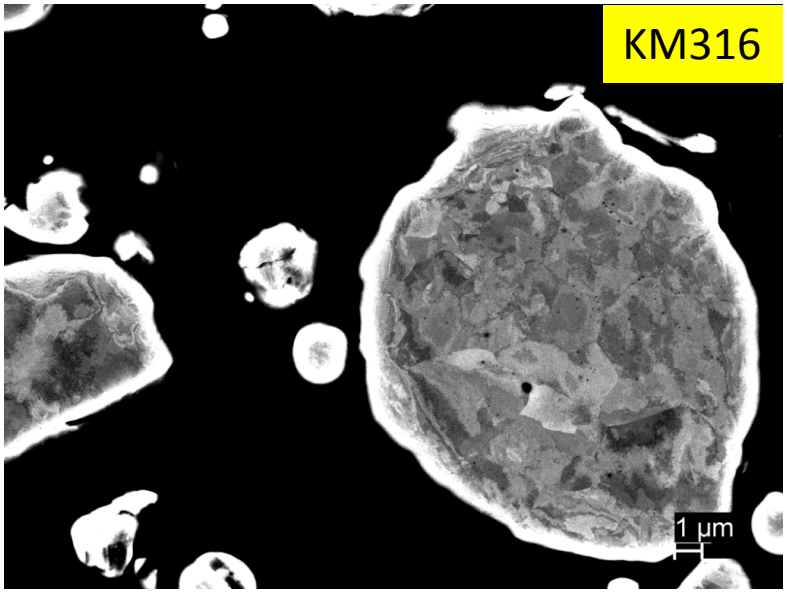

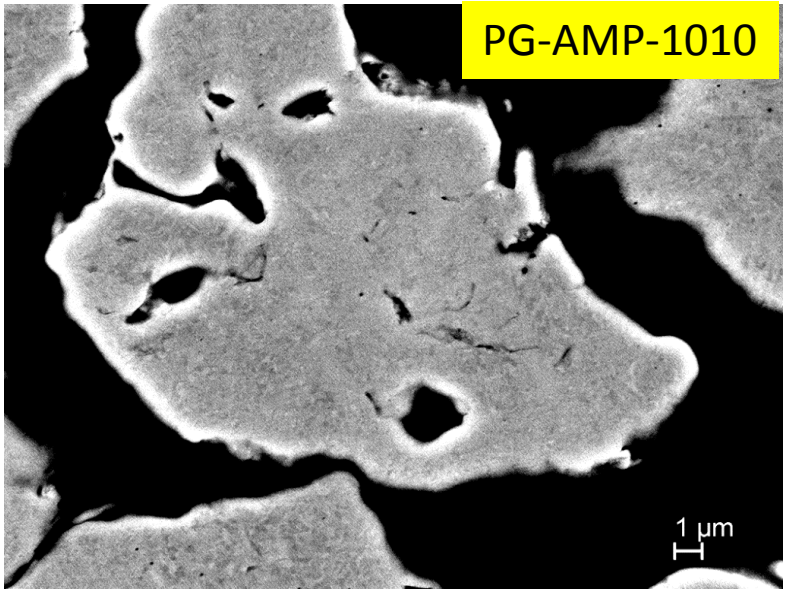

X-ray powder diffraction shows significant fractions of ferrite in the starting powders.

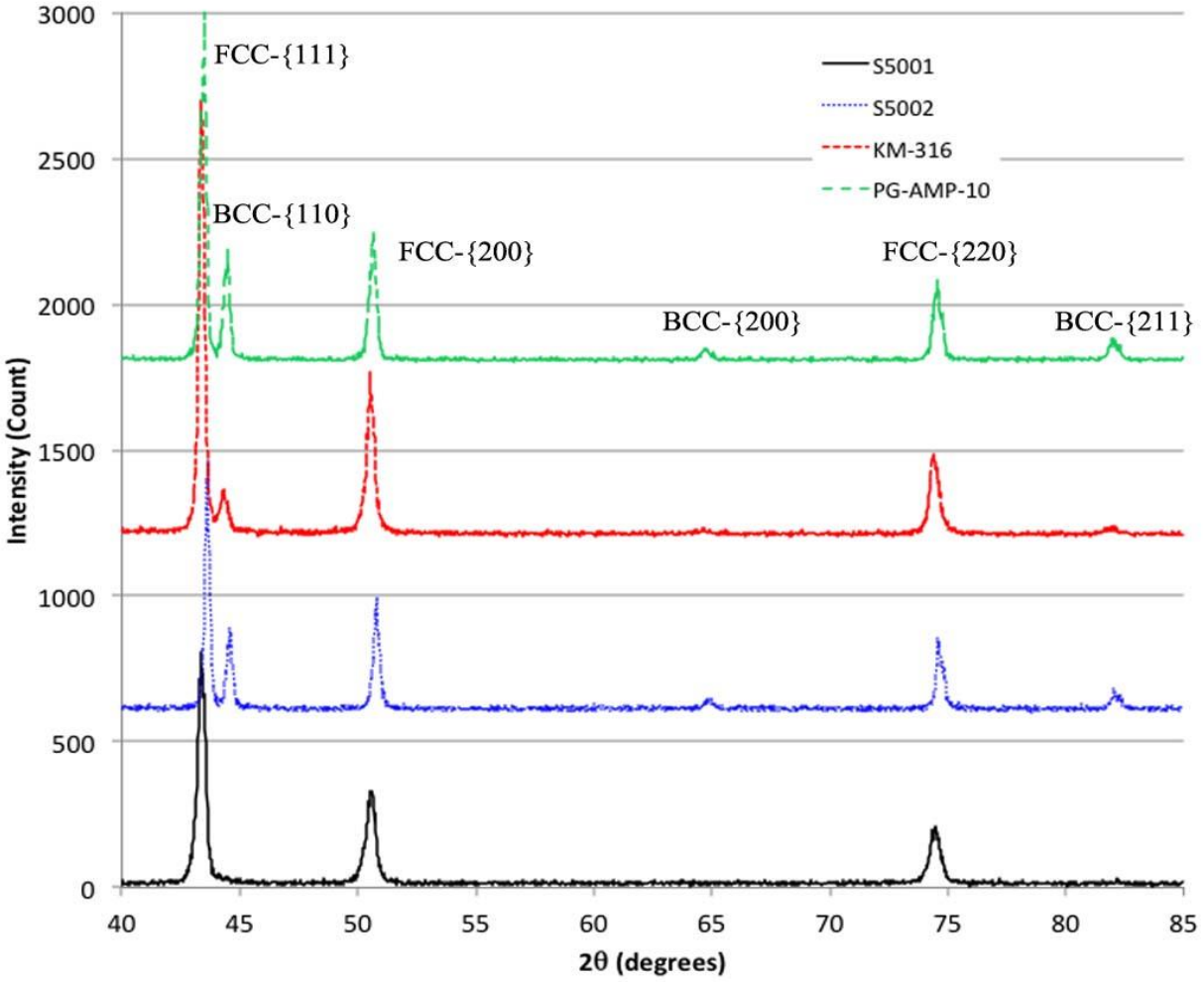

ESBD shows that the spatial distribution of ferrite also varies considerably between powders!

S5001 (304SS)

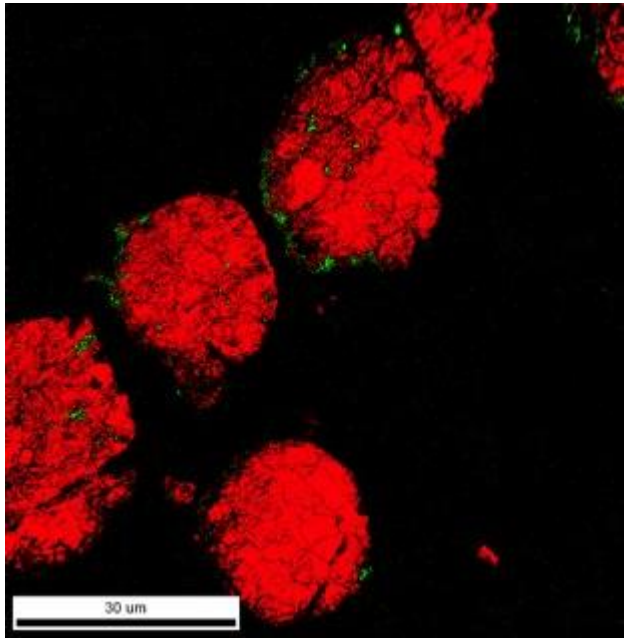

2.3% ferrite

KM316 (316LSS)

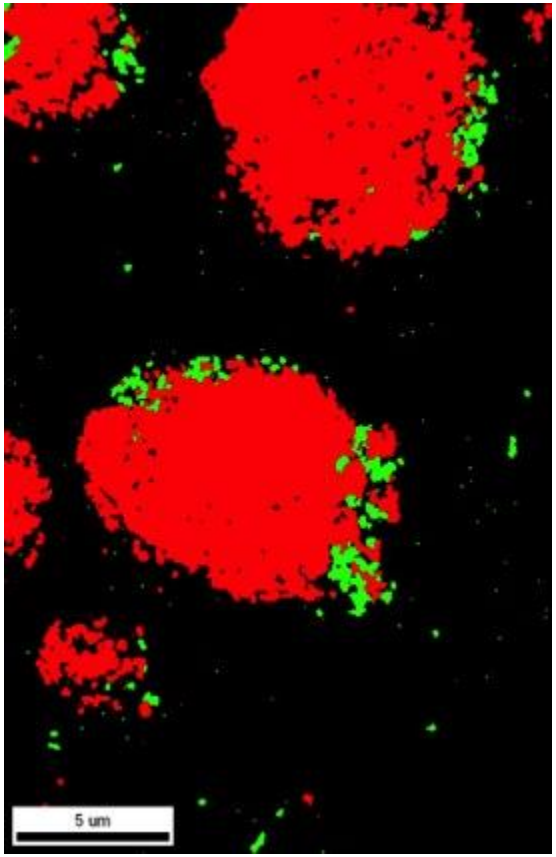

7% ferrite

PG-AMP-10 (316LSS)

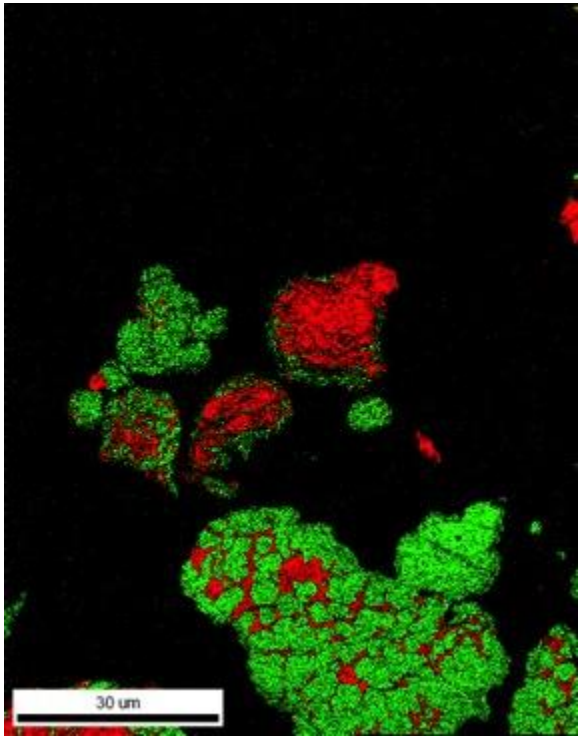

67% ferrite

austenite
ferrite

Gas Atomized Microstructures in Austenitic Stainless Steels Will Look Different

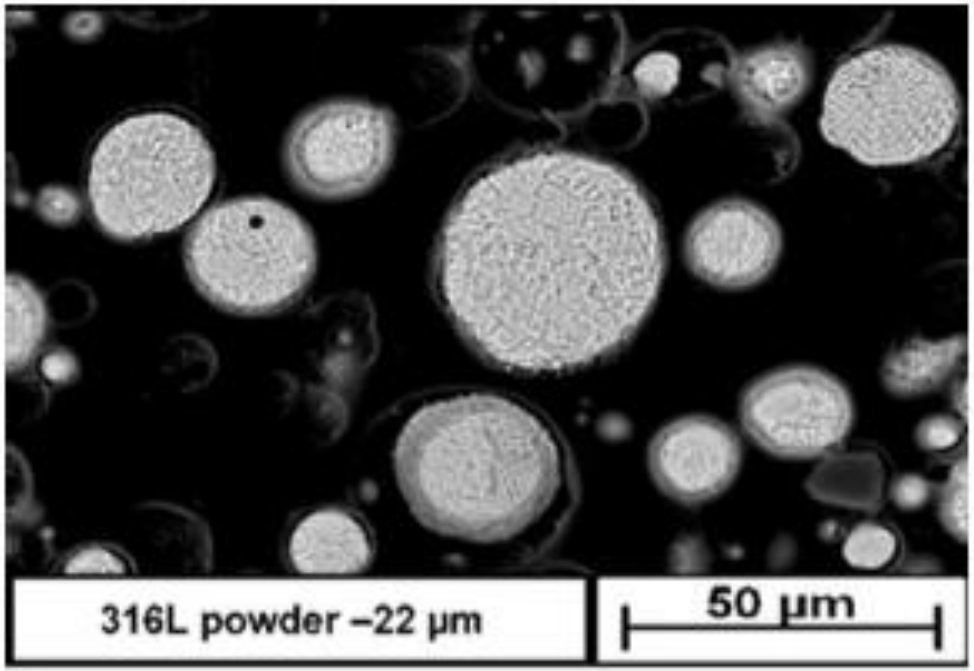

From Brochers et al., App Phys A, 2008

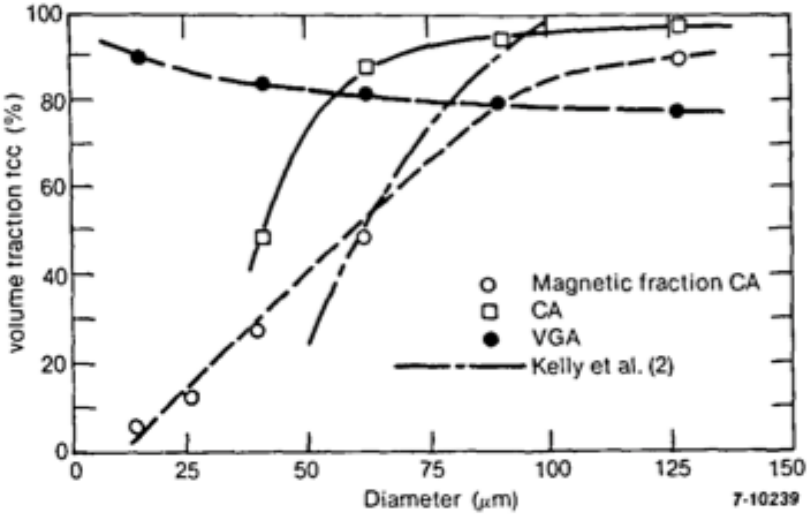

% ferrite in 304SS gas atomized powders
From Wright et al., MetTransA, 1988

- The commercial powders we have do not appear to be simply gas atomized--dendritic solidification structure absent.
- The fraction of ferrite can be very high depending upon the process used for gas atomization and the particle size
- **it is quite important to know exactly what you are spraying!

The crystallite size is in the several micron range….

PG-AMP-1010

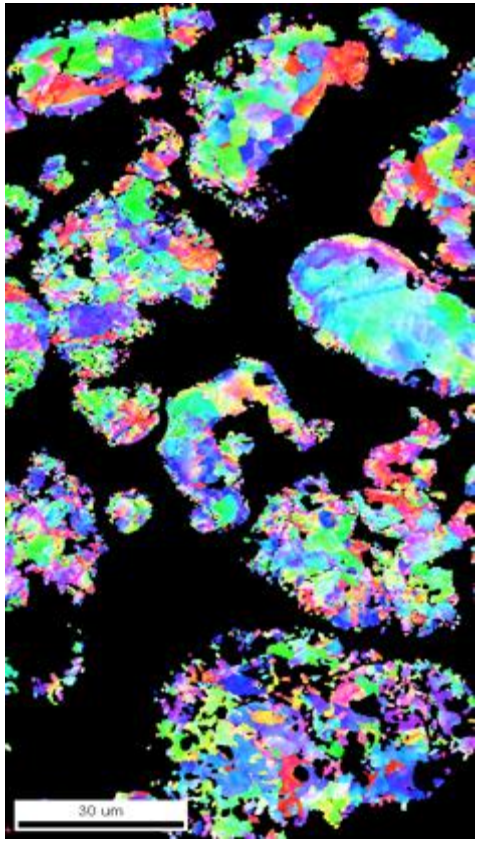

Avg. = 6.02μm

KM-316

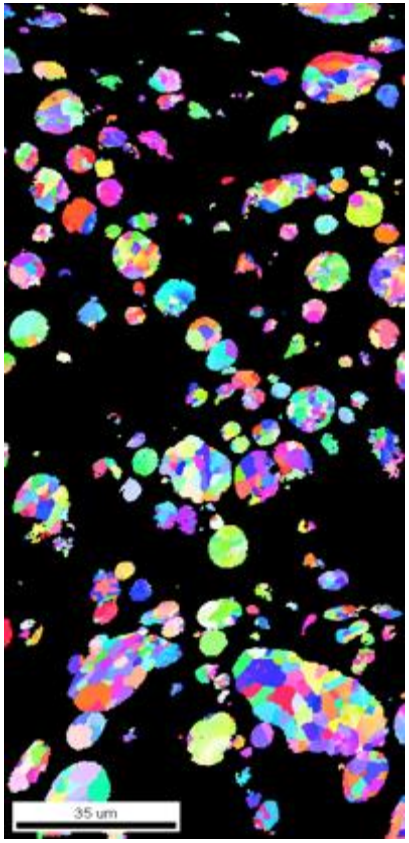

Avg. = 4.11μm

S5001

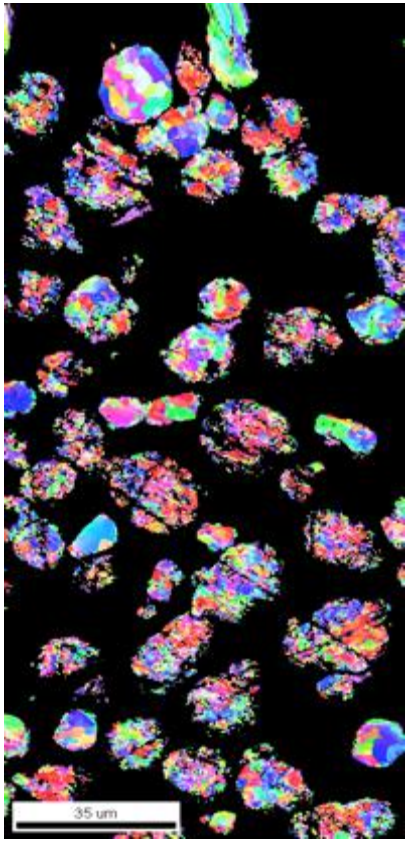

Avg. = 2.66μm

S5002

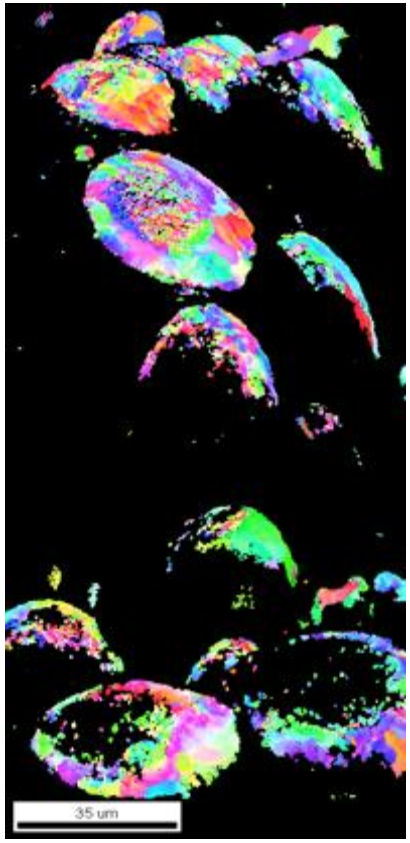

Avg. = 6.42μm

Inverse pole figure (orientation) maps from EBSD data.

Fairly high levels of intragranular misorientation in the powders…

S5001 (304SS)

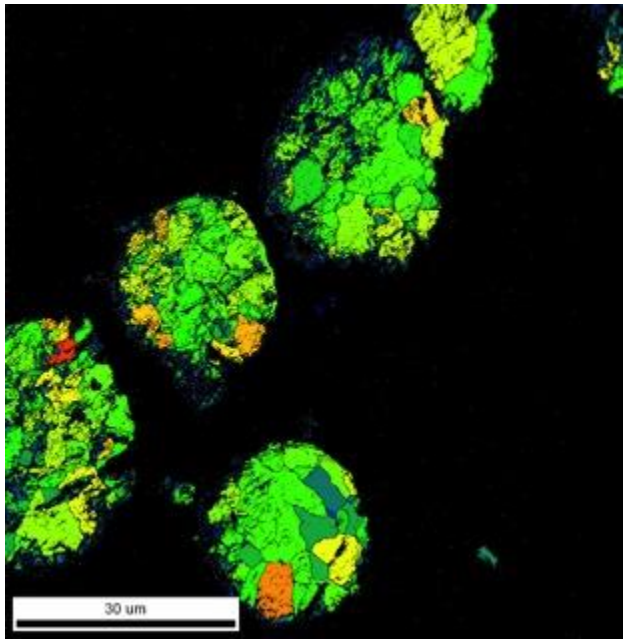

average=1.8°, max=17°

KM316 (316LSS)

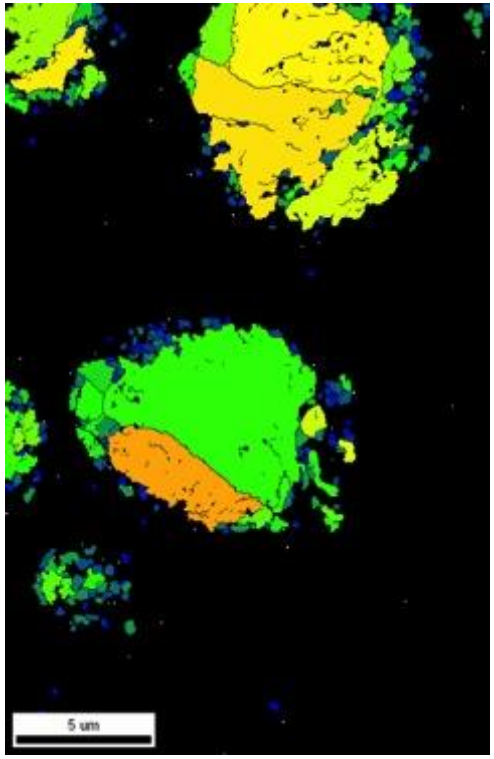

Average=2.4°, max=13°

PG-AMP-10 (316LSS)

Average=1.6°, max=15°

austenite

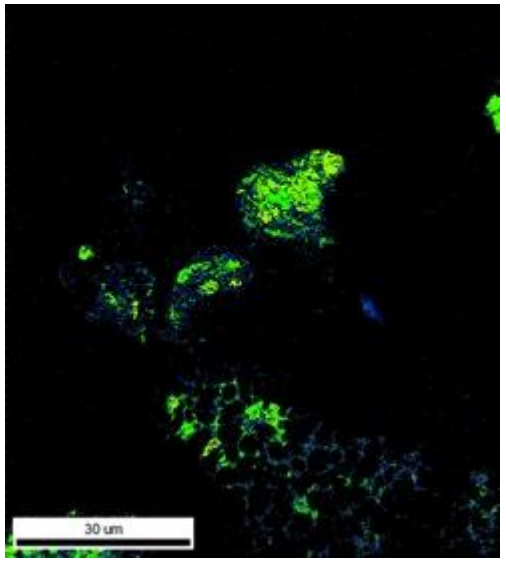

Average=1.1°, max=15°

ferrite

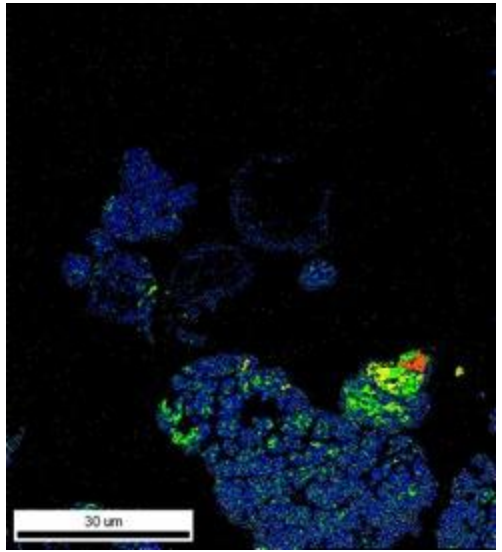

0.1° Grain Orientation Spread (GOS) 20°

High levels of GOS correlate with high levels of plastic strain…

Summary of Commercial 304/316 Powder Characteristics

	Mean Particle Size (µm)	% Ferrite (XRD)	Crystallite Size (µm)	Average GOS (°)
S5001 (304L)	19.9	~0	2.7	1.8
S5002 (316L)	45.6	50	6.4	2.4
KM-316 (316L)	17.2	23	4.1	2.4
PG-AMP-10 (316L)	61.3	46	6.0	1.6/1.1*

- Particle size fairly reasonable for cold spray deposition
- Ferrite content is quite high for the 316L powders
- Crystallite size is on the order of several microns
- The powders have been post-processed after gas atomization
  - Solidification microstructure is absent
  - Plastic deformation levels are significant→probably ball milling

Cold Spray Deposition Experiments

NPS Cold Spray System
(Centerline, Ltd.)

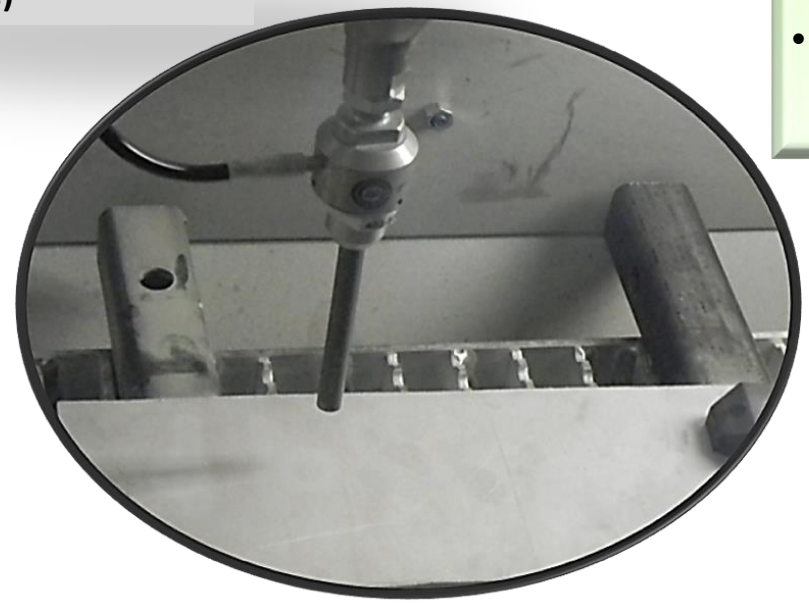

Spray Parameters

- Gas: Helium
- Gas Temperature: 250 ^{o}C
- Gas Pressure: 230 PSI (1.6 MPa)
- Substrate: gray cast iron (2” x 4” x 1/4”)
- Standoff distance: 16 mm
- Gun speed: 40 mm/sec

Cold Spray Deposition Efficiencies

Powder	N_2/450°C/250psi		He/250°C/230psi		He/175°C/325psi	
	%	mm	%	mm	%	mm
S5001	~0	0.03	11.8	1.34	4.8	1.04
S5002	~0	~0	12.3	0.71	5.2	0.57
KM-316	10.5*	0.02	41.8*	0.15	2.6*	0.03
PG	4.1	0.26	29.4	0.93	23.9	0.76

*Feed rate too low…clogging issues?

- Reasonable spray efficiencies using helium gas and higher temperature for all powders
- Nitrogen for lower pressure spray did not work well
- Both the deposition efficiency and the deposition rate are important

Basic microstructural morphology for deposits from the four powders.

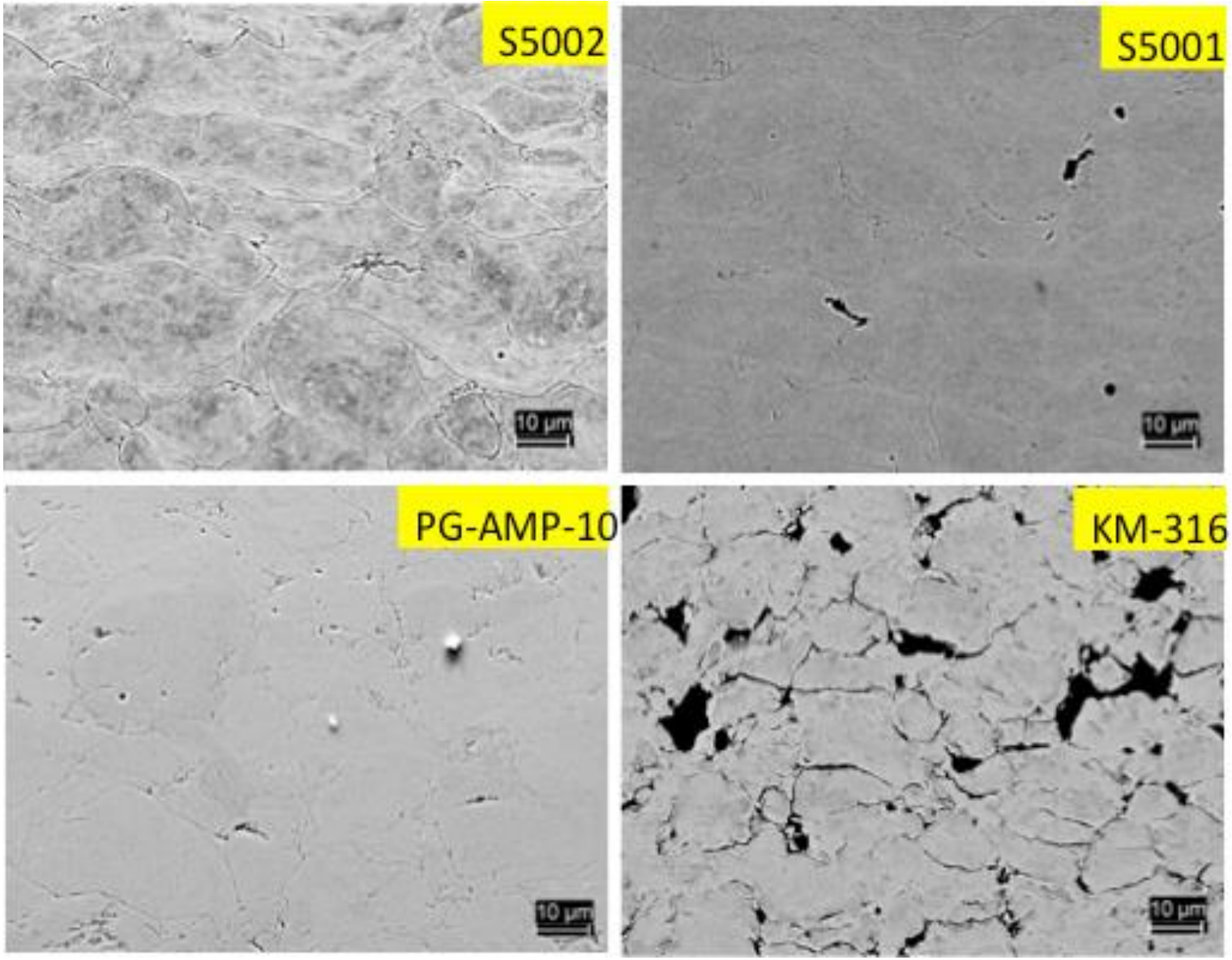

Microstructure of CS deposited shows well consolidated coatings with very fine features

CS44-2 BSE images, S5001 (304SS)

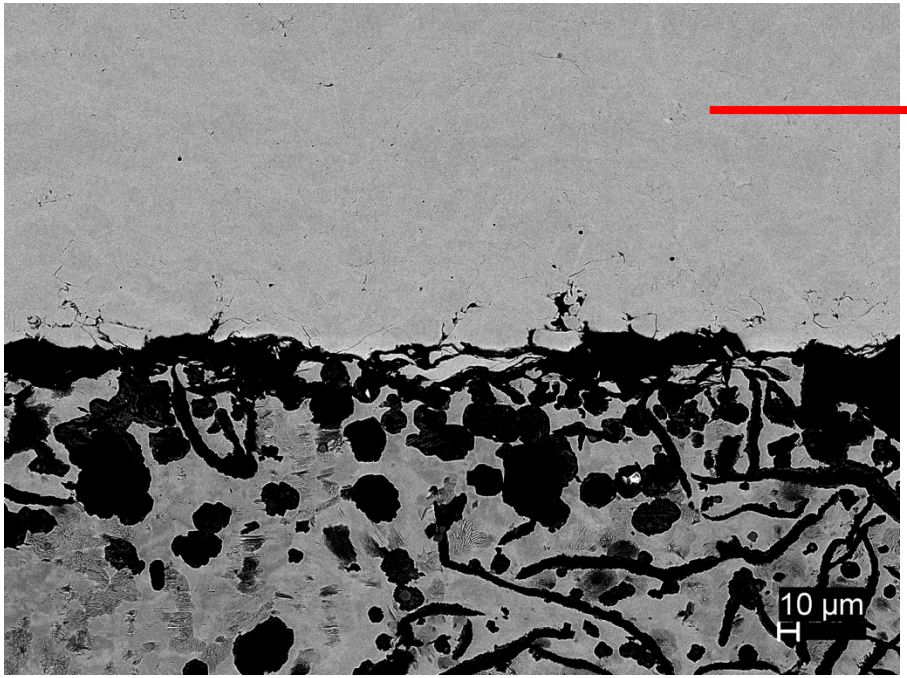

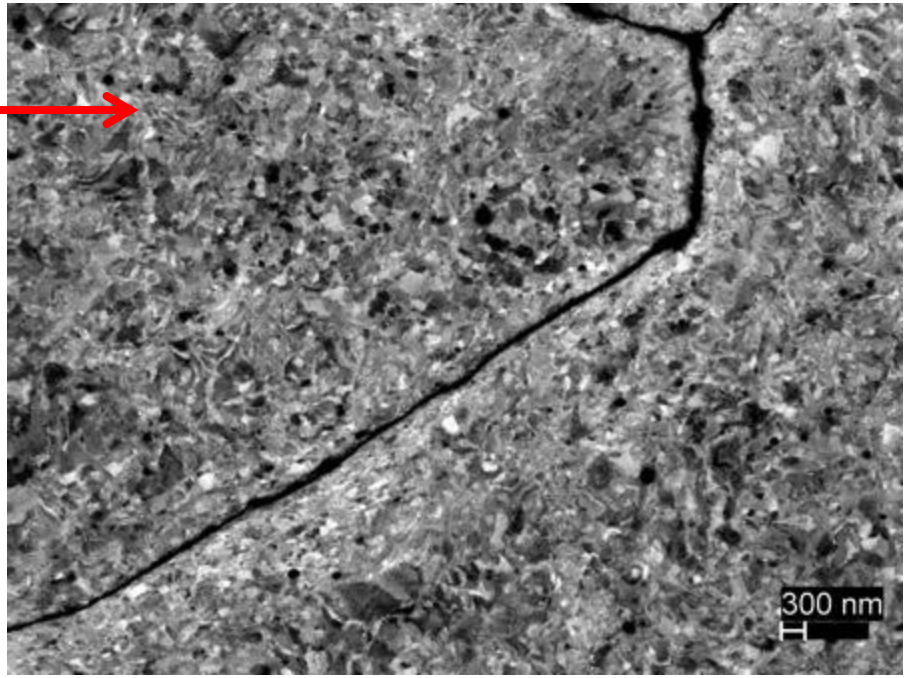

Significant (order of magnitude) reduction in crystallite size, particularly near inter-particle boundaries!

Crystallite size greatly reduced after cold spray deposition.

S5001 (304SS)

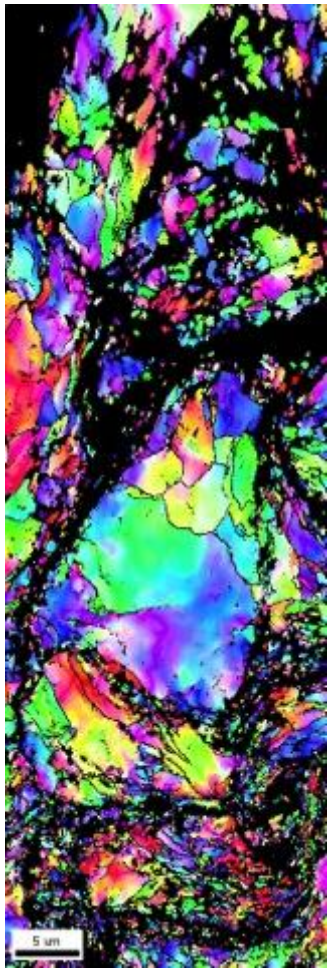

d_{avg}=0.22µm

S5002 (316LSS)

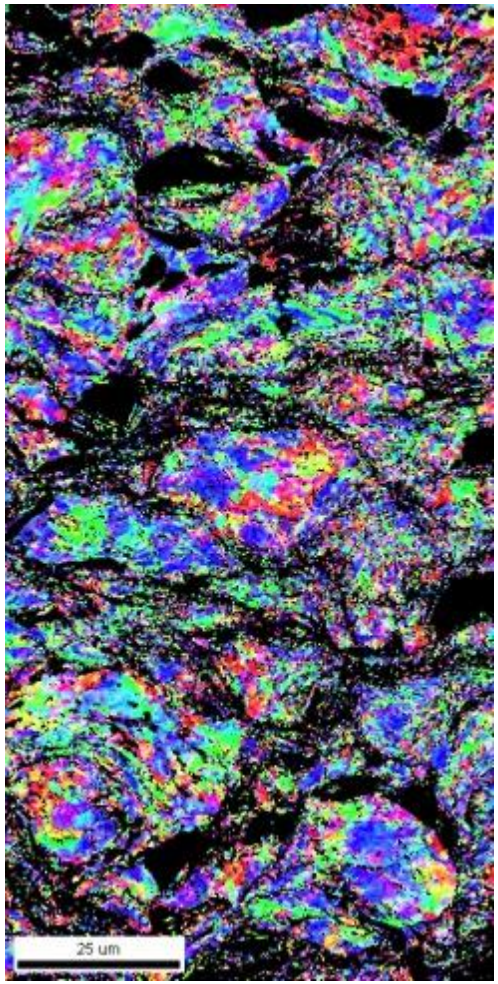

d_{avg}=0.38µm

KM316 (316LSS)

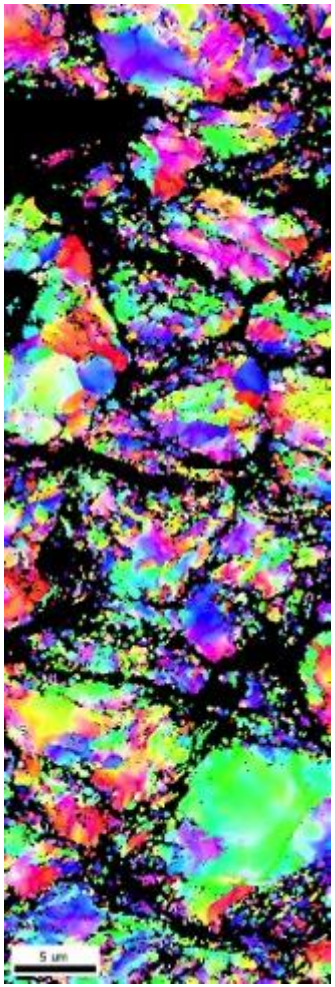

d_{avg}=0.33µm

PG-AMP-10 (316LSS)

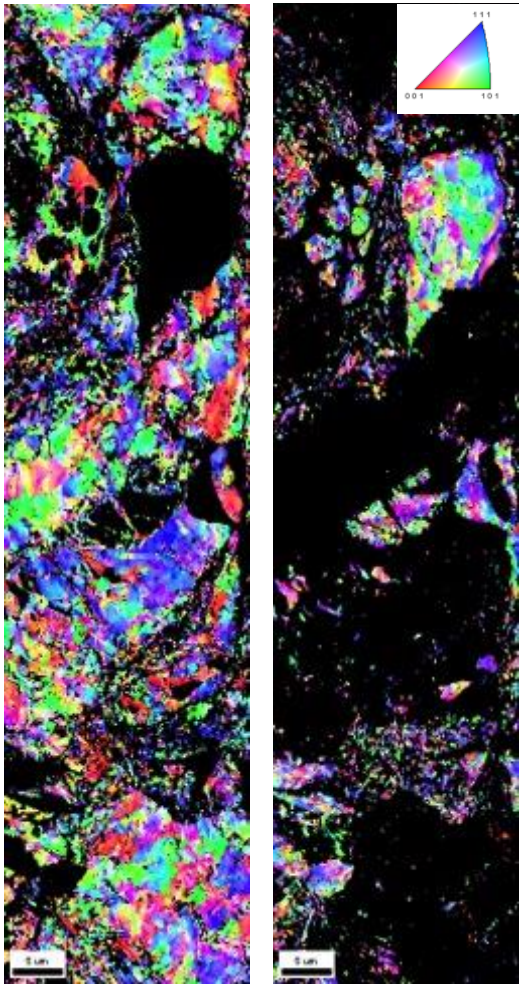

austenite d_{avg}=0.33µm (FCC),

ferrite d_{avg}=0.27µm

Electron Backscatter Diffraction-Inverse Pole Figure Maps

Ferrite content similar to starting powders.

S5001 (304SS)

S5002 (316LSS)

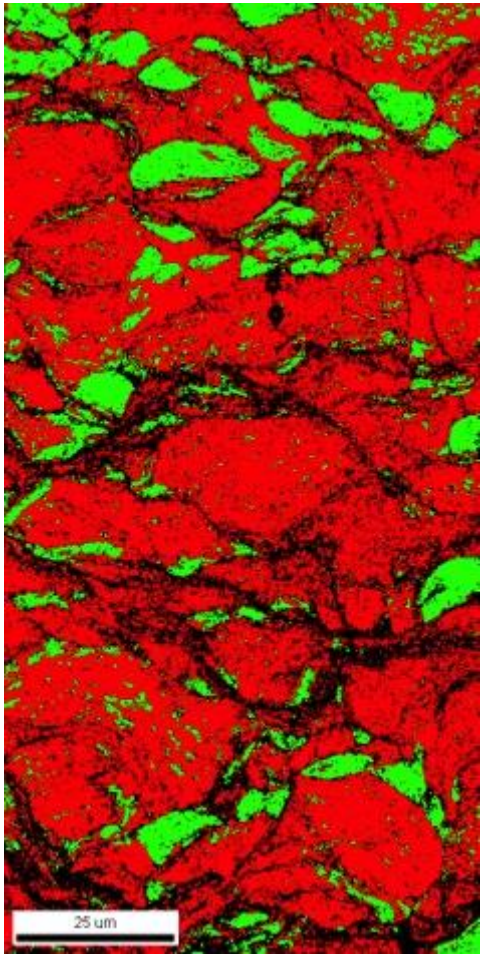

KM316 (316LSS)

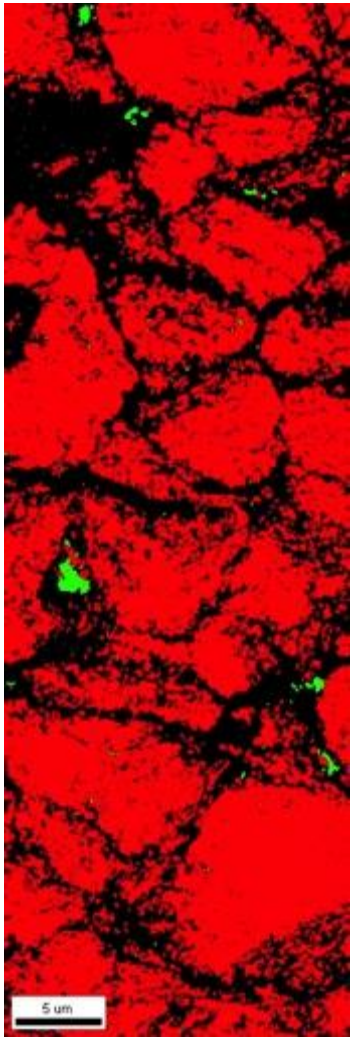

PG-AMP-10 (316LSS)

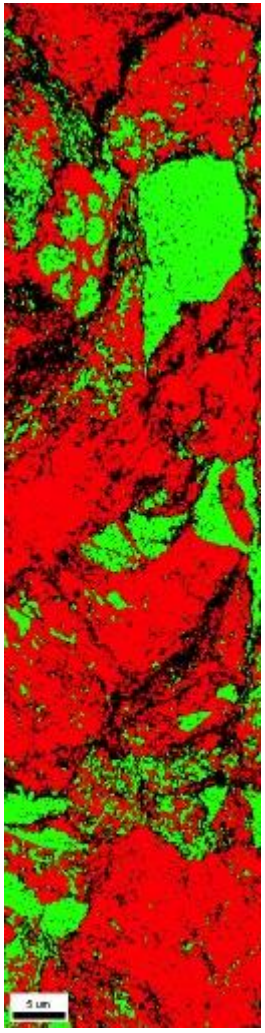

austenite
ferrite

Cold spray microstructure shows individual ferrite particles.

- S5002—finer particles seem completely comprised of ferrite
- PG-AMP-10-all austenite, all ferrite, and mixed

Intragranular misorientation increases after cold spray deposition.

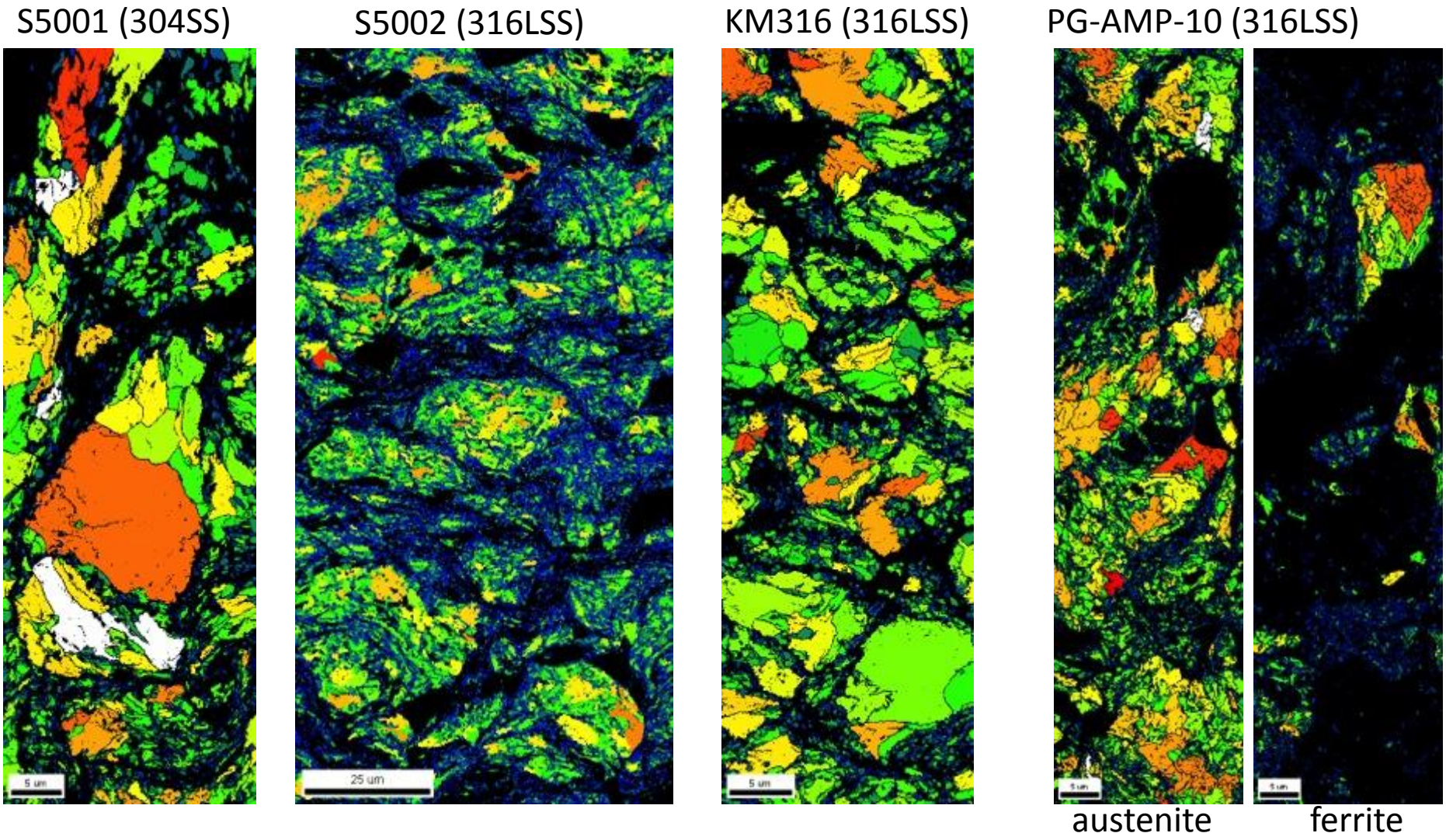

0.1° Grain Orientation Spread 20°

Note formation of composite microstructure:
Highly deformed/larger crystallite particle interior
Low deformation/small crystallite inter-particle boundaries

Vickers Hardness of CS coatings…

S5001 (304L)	S5002 (316L)	KM-316 (316L)	PG-AMP-10 (316L)
317±19 Hv	314±44 Hv	295±27 Hv	231±23 Hv

- Hardness of coatings comparable to that observed from high pressure CS of austenitic SS.
- PG-AMP-10 had the lowest hardness values by far.
- Inter-splat cracking observed in at least half of indentations

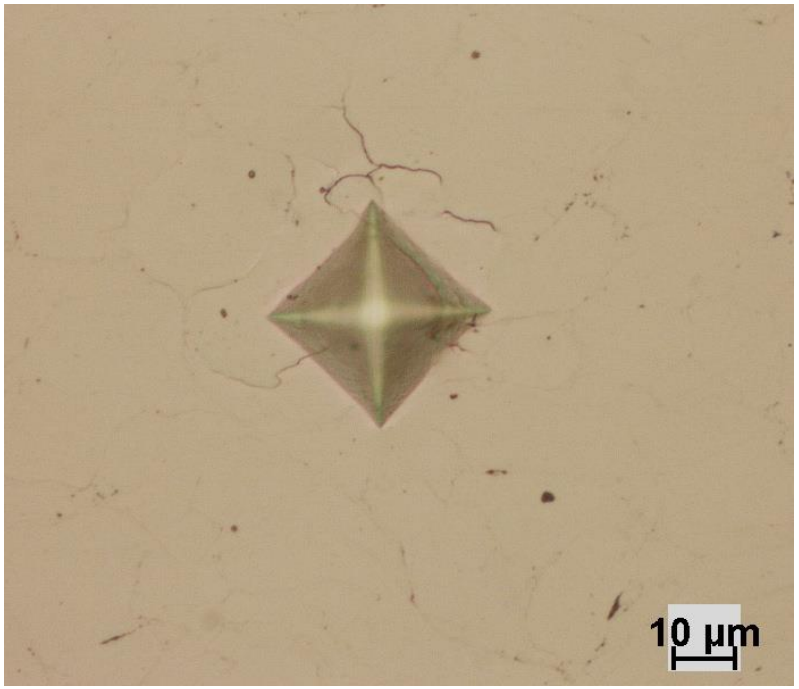

Optical micrograph of Vickers indentation in S5001 coating.

Summary of Observations for LP-Cold Spray of Commercial Austenitic Stainless Steel Powders

	DE (%)	Thicknes s (mm)	% Ferrite (EBSD)	Crystallite Size (µm)	Average GOS (°)
S5001	**11.8**	**1.34**	**~1**	**0.22**	**2.3**
S5002	**12.3**	**0.71**	**19/48+**	**0.38**	**1.7**
KM-316	**41.8**	**0.15**	**~1**	**0.33**	**2.4**
PG-AMP-10	**29.4**	**0.93**	**27/58+**	**0.33/0.22***	**2.2/1.3***

+ data from x-ray diffraction
* data for ferrite phase

- Crystallite size reduced by order of magnitude in all coatings
- Fraction ferrite mostly unchanged by CS process
- The level of plastic deformation increased after cold spray deposition-recrystallization present near inter-particle boundaries.

Summary:

- Exploring low pressure cold spray deposition of austenitic stainless steel as a means for applying corrosion resistant coating to cast iron structures.

- Identified key powder characteristics:
  - Studied four commercially available powders
  - Three of four have a good mean particle size (10-40µm)
  - The crystallite size varies somewhat from (2.7µm-6.4µm)
  - The ferrite content varies considerably!
  - There is a fair amount of plastic deformation in the particles prior to spraying

- We were able to successfully cold spray SS316L using helium gas at relatively low pressures.

- Microstructure after cold spray deposition related to powders but also changes significantly
  - Crystallite size reduced by order of magnitude in all coatings
  - Fraction ferrite mostly unchanged by CS process
  - The level of plastic deformation increased after cold spray deposition-recrystallization present near inter-particle boundaries.

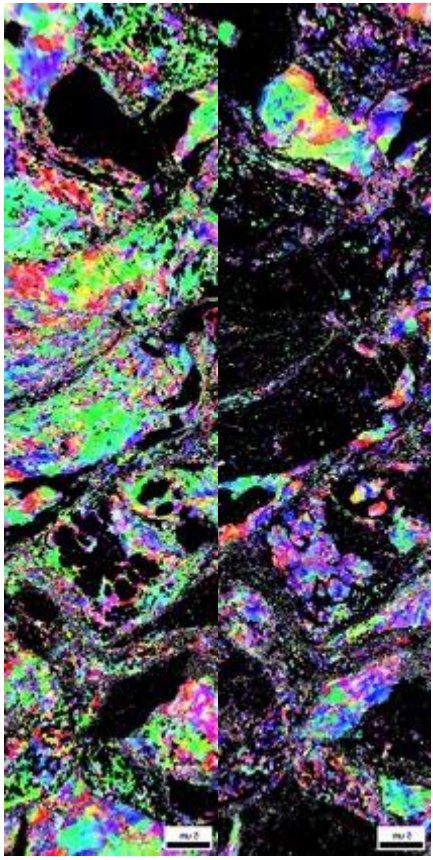

ONR Al-Cu Cold Spray Project

Luke Brewer with Al-Cu powders at NPS

- ONR (code 35)-funded collaborative project
  - NPS (Brewer, LT J. Leazer, Joe Hooper)
  - NAVAIR (Lancaster, Christophersen, Monillas, student interns)
  - NSWC-Carderock (Wolk, Bouffard)
- Successfully made Al-Cu binary composition powders
  - 2, 3, 4, and 5 wt% Cu
  - Average particle size ~20 µm
- Shipping large portion of powder to NAVAIR/NSWC-CD
- Current project thrusts
  - Powder characterization
  - Deposition studies with air and helium
  - Single particle impact experiments/simulations

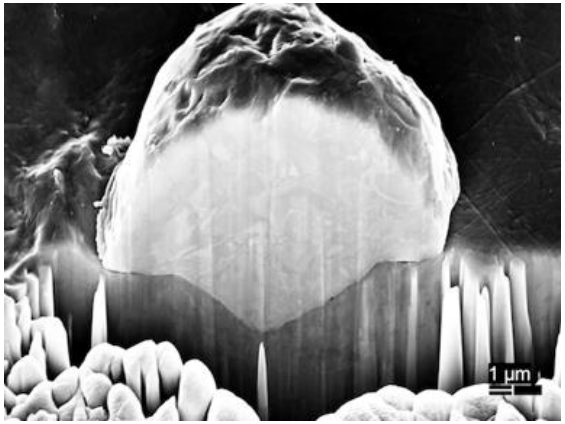

Individual splat of Cu on a polished 4340 steel surface isolated and FIB'd to examine cross section.

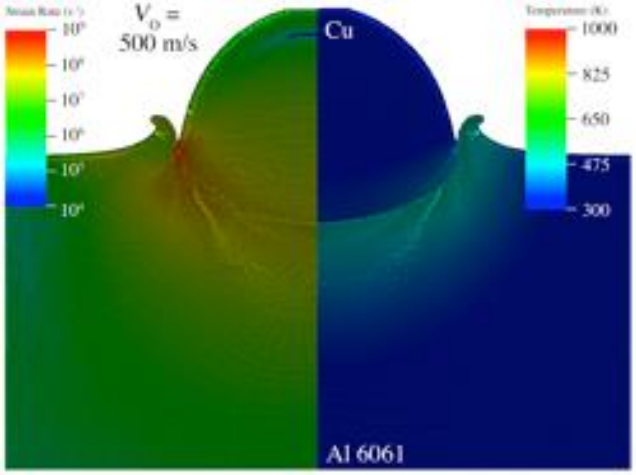

Finite element dynamics simulation of copper particle impact on AA6061.

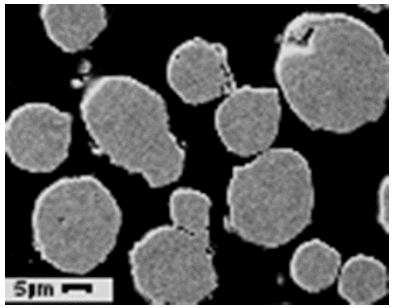

S5001

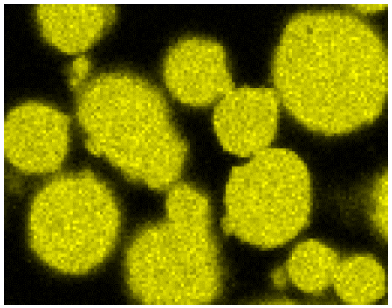

Cr K

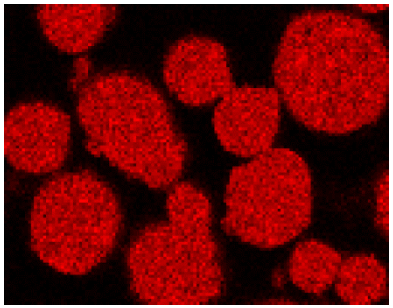

Ni K

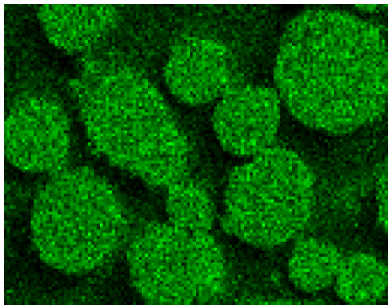

Mo L

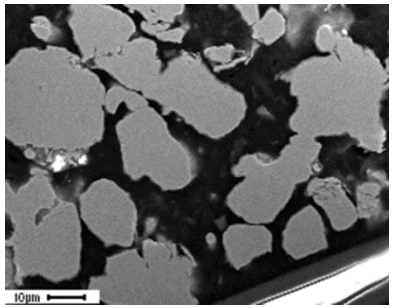

PG-AMP-10

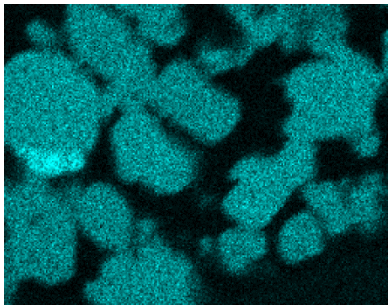

Cr K

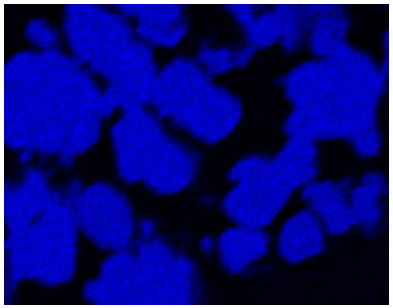

Ni K

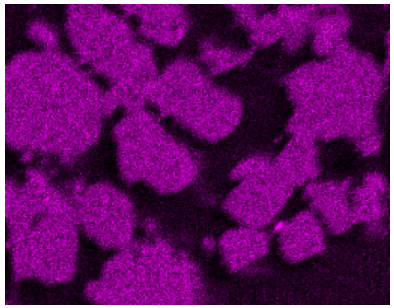

Mo L

X-ray diffraction shows that ferrite still largely present in 316L coatings after CS deposition.

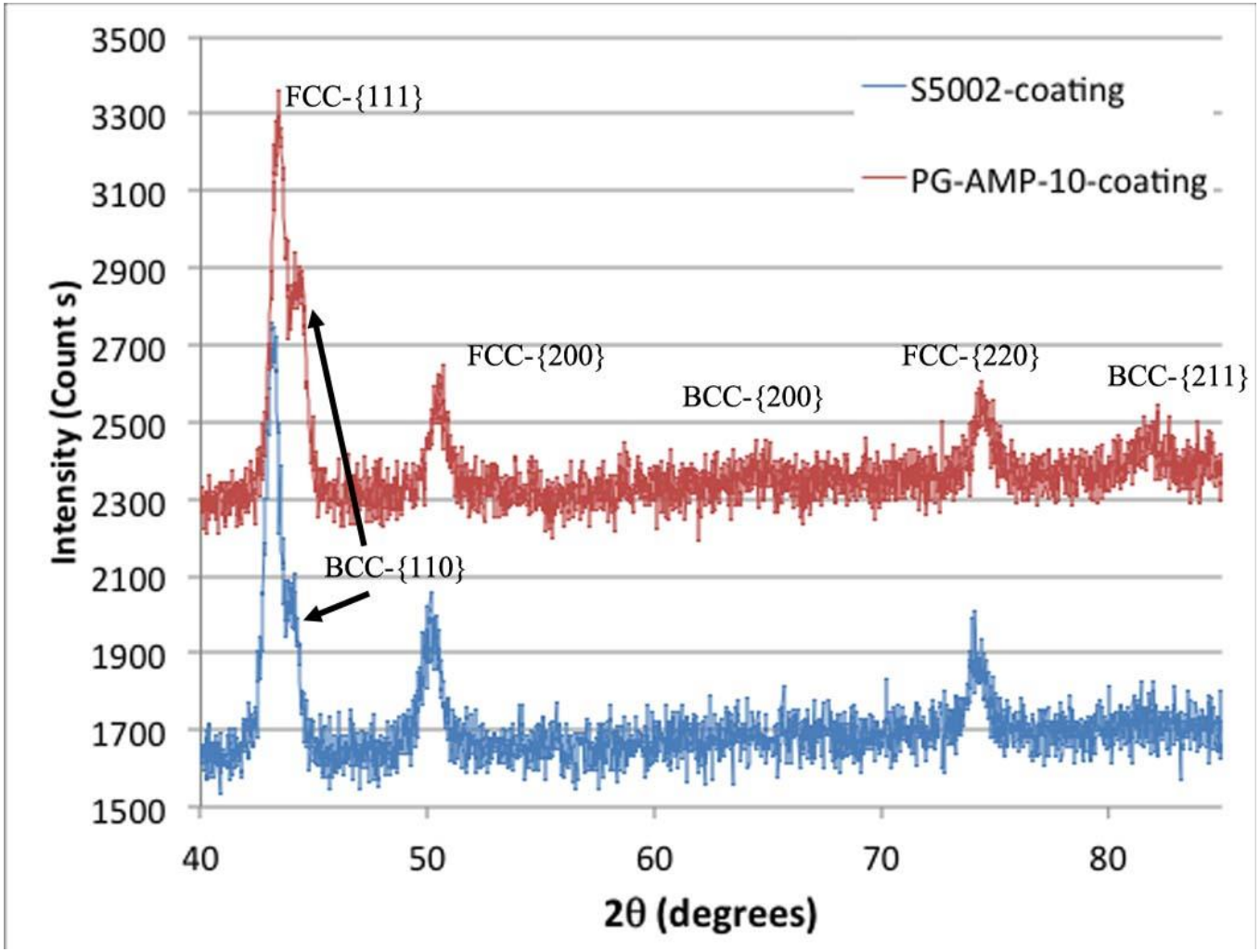

Ferrite crystallite size in PG-AMP powder is sub-micron…